Reflection Components Separation based on Chromaticity and Noise Analysis

Robby T. Tan [†] Ko Nishino [‡] Katsushi Ikeuchi [†]

Department of Computer Science [†]
The University of Tokyo
{robby,ki}@cvl.iis.u-tokyo.ac.jp

Department of Computer Science [‡]
Columbia University
kon@cs.columbia.edu

Abstract

Highlight reflected from inhomogeneous objects is the combination of diffuse and specular reflection components. The presence of highlight causes many algorithms in computer vision to produce erroneous results. To resolve this problem, a method to separate diffuse and specular reflection components is required. This paper presents such a method, particularly for objects with uniformly colored surface whose illumination color is known. The method is principally based on the distribution of specular and diffuse points in a two-dimensional chromaticity intensity space. We found that, by utilizing the space, the problem of reflection components separation can be simplified into the problem of identifying diffuse chromaticity. In our analysis, to identify the diffuse chromaticity correctly, an analysis on noise is required, since most real images suffer from it. Unlike existing methods, the proposed method is able to identify diffuse chromaticity robustly for any kind of surface roughness and light direction, without requiring diffuse-specular pixel segmentation. In addition, to enable us to obtain a pure-white specular component, we present a handy normalization technique that does not require approximated linear basis functions.

1 Introduction

In the field of computer vision, it is well known that the presence of specular reflection causes many algorithms to produce erroneous results. Many algorithms in the field assume diffuse only reflection and deem specular reflection as outliers. To resolve the problem, a method to separate diffuse and specular reflection component is required. Once this separation has been accomplished, besides obtaining diffuse only reflection, knowledge of specular reflection component can be advantageous, since it conveys useful information about the surface properties such as microscopic roughness.

Many methods have been proposed to separate reflection components. Wolff et al. [14] introduced the use of polarizing filter to obtain specular components. Nayar et al. [9] extended this work by considering colors of an object instead of using a polarizing filter alone. Generally, methods using polarizing filters are sufficiently accurate to separate reflection components; however, using such additional devices is impractical in some circumstances. Sato et al. [11] introduced a four-dimensional space, temporal-color space, to analyze the diffuse and specular reflections based solely on color. While their method requires dense input images with variation of illuminant directions, it has the ability to separate the reflection components locally, since each pixel's location contains information of diffuse and specular reflections. Lin et al. [8], instead of using dense images, used sparse images under different illumination positions to resolve the separation problem. They used an analytical method that combines the finite dimensional basis model and dichromatic model to form a closed form equation, by assuming that the sensor sensitivity is narrowband. Their method also solves reflection component separation locally. Other methods using multiple images can be found in the literature [10, 6, 7].

Shafer [12], who proposed the dichromatic reflection model, was one of the early researchers who used a single colored image as input. He proposed a separation method based on parallelogram distribution of colors in RGB space. Klinker et al. [4] extended this method by introducing a T-shaped color distribution, which was composed of reflectance and illumination color vectors. Separating these vectors caused the reflection equation to become a closed-form equation. Unfortunately, for most real images, this T shape is hardly extractable due to noise, etc. Bajscy et al. [1] proposed a different approach by introducing a three dimensional space composed of lightness, saturation and hue. In their method, the input image whose illumination color is known has to be neutralized to pure-white illumination using a linear basis functions operation. For every neutralized pixel, the weighting factors of the surface reflectance basis functions are projected into the three-dimensional space, where specular and diffuse reflections can be identifiable, due to the differences in their saturation values. Although this method is more accurate than the method of Klinker et al. [4], it requires correct specular-diffuse pixel segmentation, which is dependent on camera parameters.

In this paper, our goal is to separate the reflection components of uniformly colored surfaces from a single input

image without specular-diffuse pixel segmentation. To accomplish this, we base the method on chromaticity, particularly on the distribution of specular and diffuse points in the chromaticity intensity space. Briefly, the method is as follows. Given a single uniformly colored image taken under uniformly colored illumination, we first identify the diffuse pixel candidates based on color ratio and noise analysis, particularly camera noise. We normalize both input image and diffuse pixel candidates simply by dividing their pixels values with known illumination chromaticity. To obtain illumination chromaticity from a uniformly colored surface, color constancy algorithms proposed by Tan et al. [13] can be used. From the normalized diffuse candidates, we estimate the diffuse chromaticity using histogram analysis. By having the normalized image and the normalized diffuse chromaticity, the separation can be done straightforwardly using a *specular-to-diffuse mechanism*, a new mechanism which we introduce. In the last step, we renormalize the reflection components to obtain the actual reflection components.

There are several advantages of our method: first, diffuse chromaticity detection is done without requiring segmentation process. Second, the method uses simple and hands-on illumination color normalization. Third, it produces robust and accurate results for all kinds of surface roughness and light directions.

The rest of the paper is organized as follows. In Section 2, we discuss image color formation of dielectric inhomogeneous objects. In Section 3, we explain the method in detail, describing the derivation of the theory and the algorithm for separating diffuse and specular reflection components. We provide a brief description of the implementation of the method and experimental results for real images, in Section 4. Finally in Section 5, we offer our conclusions.

2 Reflection Models

Considering the dichromatic reflection model and image formation of a digital camera, we can describe image intensity as:

$$I_c(\mathbf{x}) = w_d(\mathbf{x}) \int_\Omega S(\lambda)E(\lambda)q_c(\lambda)d\lambda + w_s(\mathbf{x}) \int_\Omega E(\lambda)q_c(\lambda)d\lambda \quad (1)$$

where $\mathbf{x} = \{x, y\}$, the two dimensional image coordinates, q_c is the three-element-vector of sensor sensitivity and c represents the type of sensors (r, g, and b). $w_d(\mathbf{x})$ and $w_s(\mathbf{x})$ are the weighting factors for diffuse and specular reflection, respectively; their values depend on the geometric structure at location $\mathbf{x}$. $S(\lambda)$ is the diffuse spectral reflectance function. $E(\lambda)$ is the spectral energy distribution function of illumination. These two spectral functions are independent of the spatial location ($\mathbf{x}$) because we assume a uniform surface color as well as a uniform illumination color. The integration is done over the visible spectrum (Ω). Note that we ignore the camera gain and camera noise in the above model, and assume that the model follows the neutral interface reflection (NIR) assumption [5].

For the sake of simplicity, Equation (1) can be written as:

$$I_c(\mathbf{x}) = w_d(\mathbf{x})B_c + w_s(\mathbf{x})G_c \quad (2)$$

where $B_c = \int_\Omega S_d(\lambda)E(\lambda)q_c(\lambda)d\lambda$; and $G_c = \int_\Omega E(\lambda)q_c(\lambda)d\lambda$. The first part of the right side of the equation represents the diffuse reflection component, while the second part represents the specular reflection component.

Chromaticity Our separation method is also based on chromaticity, which is defined as:

$$\sigma_c(\mathbf{x}) = \frac{I_c(\mathbf{x})}{\Sigma I_i(\mathbf{x})} \quad (3)$$

where $\Sigma I_i(\mathbf{x}) = I_r(\mathbf{x}) + I_g(\mathbf{x}) + I_b(\mathbf{x})$.

By considering the chromaticity definition in Equation (3), for diffuse only reflection component ($w_s = 0$), the chromaticity becomes independent from the diffuse geometrical parameter w_d. We call this *diffuse chromaticity* (Λ_c) with definition:

$$\Lambda_c = \frac{B_c}{\Sigma B_i} \quad (4)$$

On the other hand, for specular only reflection component ($w_d = 0$), the chromaticity is independent from the specular geometrical parameter (w_s), which we call *specular chromaticity* (Γ_c):

$$\Gamma_c = \frac{G_c}{\Sigma G_i} \quad (5)$$

By considering Equation (4) and (5), consequently Equation (2) can be written as:

$$I_c(\mathbf{x}) = m_d(\mathbf{x})\Lambda_c + m_s(\mathbf{x})\Gamma_c \quad (6)$$

where

$$m_d(\mathbf{x}) = w_d(\mathbf{x})\Sigma B_i \quad (7)$$
$$m_s(\mathbf{x}) = w_s(\mathbf{x})\Sigma G_I \quad (8)$$

We can also set $\Sigma\sigma_i = \Sigma\Lambda_i = \Sigma\Gamma_i = 1$, without loss of generality. As a result, we have three types of chromaticity: image chromaticity (σ_c), diffuse chromaticity (Λ_c) and specular chromaticity (Γ_c). The image chromaticity is directly obtained from the input image using Equation (3).

3 Separation Method

In this section, we first deal with input images that have a pure-white specular component ($\Gamma_r = \Gamma_g = \Gamma_b$). Then, we encounter more realistic images where $\Gamma_r \neq \Gamma_g \neq \Gamma_b$ by utilizing a normalization technique.

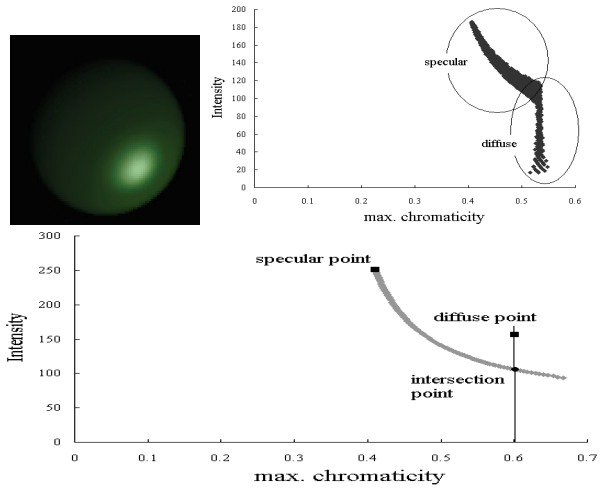

Figure 1: (a) Synthetic image (b) The projection of the synthetic image pixels into the chromaticity intensity space (c) Specular-to-diffuse mechanism. The intersection point is equal to the diffuse component of the specular pixel

3.1 Specular-to-diffuse mechanism

The algorithm of *specular-to-diffuse mechanism* is based on maximum chromaticity and intensity values of specular and diffuse pixels. We define *maximum chromaticity* as:

$$\tilde{\sigma}(\mathbf{x}) = \frac{max(I_r(\mathbf{x}), I_g(\mathbf{x}), I_b(\mathbf{x}))}{\Sigma I_i(\mathbf{x})} \tag{9}$$

By assuming a uniformly colored surface lit with a single colored illumination, in a two-dimensional space: chromaticity intensity space, where its x-axes representing $\tilde{\sigma}$ and its y-axes representing $\tilde{I}$ (with $\tilde{I}$ is the image intensity of certain color channel that is the same to the color channel of $\tilde{\sigma}$), the diffuse pixels are always located at the right side of the specular pixels, due to the maximum chromaticity definition in Equation (9). Also, using either the chromaticity or the maximum chromaticity definition, the chromaticity values of the diffuse points will be constant, regardless of the variance of m_d. In contrast, the chromaticity values of specular points will vary with regard to the variance of m_s, as shown in Figure 1.b. From these different characteristics of specular and diffuse points in the chromaticity intensity space, we devised the specular-to-diffuse mechanism. The details are as follows.

When two pixels, a specular pixel $I_c(\mathbf{x_1})$ and a diffuse pixel $I_c(\mathbf{x_2})$, with the same surface color are projected into the chromaticity intensity space, the maximum chromaticity ($\tilde{\sigma}$) of the diffuse point will be bigger than that of the specular point. If the color of the specular component is pure white: $\Gamma_r(\mathbf{x_1}) = \Gamma_g(\mathbf{x_1}) = \Gamma_b(\mathbf{x_1})$, by subtracting all channels of the specular pixel's intensity using a small scalar number iteratively, and then projecting them into the space, we will find that the points form a curved line, as shown in Figure 1.c. This curved line follows the below Equation (see the Appendix for complete derivation):

$$\tilde{I} = m_d(\tilde{\Lambda} - \tilde{\Gamma})(\frac{\tilde{\sigma}}{\tilde{\sigma} - \tilde{\Gamma}}) \tag{10}$$

where $\tilde{\Lambda}$ and $\tilde{\Gamma}$ are the diffuse chromaticity and specular chromaticity of certain color channel that is the same to the color channel of $\tilde{\sigma}$, respectively.

In Figure 1.c. we can observe that a certain point in the curved line intersects with a vertical line representing the chromaticity value of the diffuse point. At this intersection, m_s of the specular pixel equals zero. Consequently, the intersection point becomes crucial, because the point indicates the diffuse component of the specular pixel. Mathematically, the intersection point (the diffuse component of the specular pixel) can be calculated as follows.

As mentioned in Section 2, the sum of illumination chromaticity for all color channels is equal to one ($\Sigma\Gamma_i = 1$), hence if $\Gamma_r = \Gamma_g = \Gamma_b$ then $\Gamma_c = \frac{1}{3}$. From Equation (8), we can obtain that m_d equals to ΣI_i^{diff} (the total intensity of diffuse component for all color channels), because $w_d \Sigma B_i$ is identical to ΣI_i^{diff}. Therefore, based on Equation (10) we can derive the total diffuse intensity of specular pixels as:

$$\Sigma I_i^{diff} = \frac{\tilde{I}(3\tilde{\sigma} - 1)}{\tilde{\sigma}(3\tilde{\Lambda} - 1)} \tag{11}$$

To calculate $\Sigma I_i^{diff}(\mathbf{x_1})$, the value of $\tilde{\Lambda}(\mathbf{x_1})$ is required. This value can be obtained from the diffuse pixel $I_c(\mathbf{x_2})$, since if the two pixels have the same surface color, then $\tilde{\Lambda}(\mathbf{x_1}) = \tilde{\sigma}(\mathbf{x_2})$. Having calculated $\Sigma I_i^{diff}(\mathbf{x_1})$, the specular component is obtained using:

$$m_s(\mathbf{x_1}) = \frac{\Sigma I_i(\mathbf{x_1}) - \Sigma I_i^{diff}(\mathbf{x_1})}{3} \tag{12}$$

Finally, by subtracting the specular component (m_s) from the specular pixel intensity (I_c) the diffuse component becomes obtainable:

$$I_c^{diff}(\mathbf{x_1}) = I_c(\mathbf{x_1}) - m_s(\mathbf{x_1}) \tag{13}$$

Based on the above mechanism, therefore the problem of reflection component separation can be simplified into the problem of finding diffuse chromaticity. For synthetic images, which have no noise, the diffuse chromaticity values are constant and thus trivial to find. Figure 1.b, shows the distribution of synthetic image pixels in the chromaticity-intensity space. By considering the maximum chromaticity definition (9), we can obtain the diffuse chromaticity from the biggest chromaticity value (the extreme right of the point cloud). Then, we can accomplish the separation in straightforward manner using the above mechanism with regard to the diffuse chromaticity. Figure 2.b∼c show the separation result.

For real images, unfortunately, instead of forming a constant chromaticity values, the diffuse pixels' chromaticity varies within a considerably wide range (Figure 2.e). This

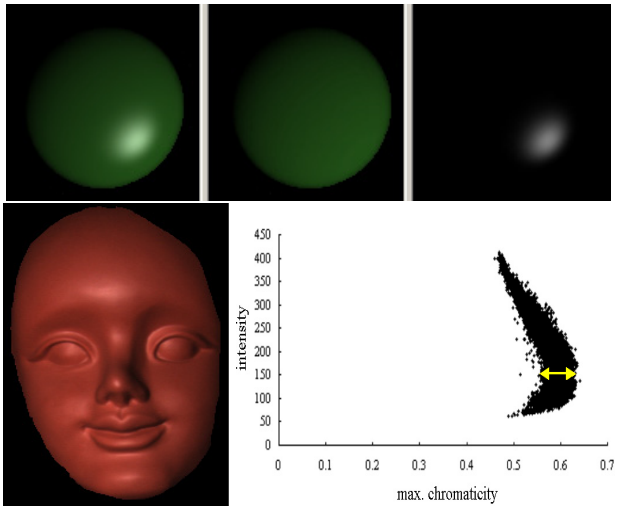

Figure 2: (a) Synthetic image (b) Diffuse component (c) Specular component (d) The projection of synthetic image pixel into chromaticity-intensity space (e) The projection of real image pixel into chromaticity-intensity space

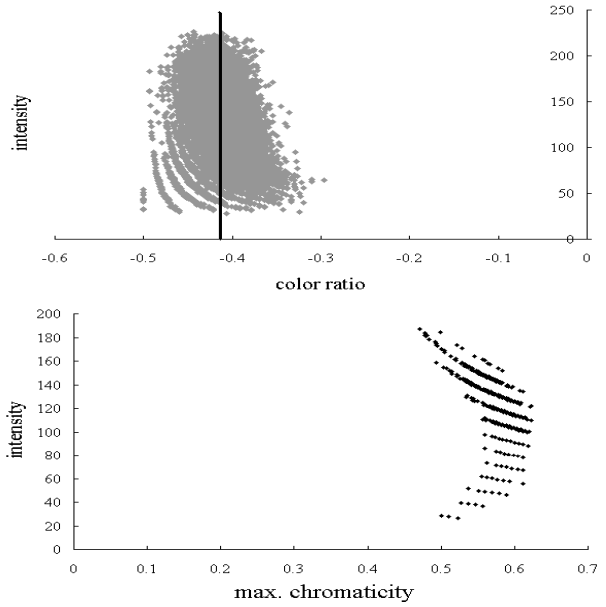

Figure 3: (a) The projection of the pixels of Figure 2.d into u-intensity space (b) Result of plotting pixels obtained from one straight line in u-intensity space (vertical line in Figure a) into chromaticity intensity space.

is due to imaging noises and surface non-uniformity (although human perception perceives a uniform color, in fact in the real world, there is still surface non-uniformity due to dust, imperfect painting, etc.). Therefore, to correctly and robustly obtain the diffuse chromaticity, we must include those noises in our analysis.

Note that the specular-to-diffuse mechanism requires linearity between the camera output and the flux of incoming light intensity. And, in this paper, the mechanism will be used for two purposes: first, to identify diffuse candidates and second, to calculate diffuse components of specular pixels.

3.2 Color Ratio and Noise Analysis

In order to analyze both camera noise and surface non-uniformity, we first need to group image pixels based on their color ratio values. We define color ratio as:

$$u = \frac{I_r + I_b - 2I_g}{I_g + I_b - 2I_r} \tag{14}$$

the location parameter $\mathbf{x}$ is removed, since we work on each pixel independently. For pure-white specular reflection component where $\Gamma_r = \Gamma_g = \Gamma_b$, u can be expressed as: $u = \frac{\Lambda_r + \Lambda_b - 2\Lambda_g}{\Lambda_g + \Lambda_b - 2\Lambda_r}$. One of the important properties of u is its independence from shadows, shading and specularity. The independence from shadow is fulfilled if the ambient illumination has the same spectral energy distribution to the direct illumination [2].

Using a color ratio (u) definition, we create a two-dimensional space: u-intensity space, with u as its x-axis and $\tilde{I}$ as its y-axes. By projecting all pixels of a real image into this space, we obtain a cloud of points as shown in Figure 3.a. Ideally, if the surface color is perfectly unique and there is no noise from the camera, we should observe only a single straight line in this space. However, as can be seen in the figure, this does not hold true for real images. This is mainly due to the slight variation of surface color and illumination color, which are insensitive to human eyes, as well as the noise produced through the camera sensing process. In our analysis, however, we assume the variance of illumination color is small, and neglect it. Thus, the variance of the color ratio in the space is caused by surface non-uniformity and camera noise.

By considering the camera noise, Equation (6) becomes:

$$I_c(\mathbf{x}) = \Big[m_d(\mathbf{x})\Lambda_c + m_s(\mathbf{x})\Gamma_c\Big]\theta_c(\mathbf{x}) + \phi_c(\mathbf{x}) \tag{15}$$

where $\theta_c(\mathbf{x})$ and $\phi_c(\mathbf{x})$ are the first and second types of camera noise in the three sensor channels, respectively. The two types of camera noise depend on the position of the image $\mathbf{x}$, indicating that the noise can be different for each location in the image. The above model is a simplification of a more complex model proposed by Healey et al. [3]. According to that model, there are two types of camera noise, namely, noise that is dependent on incoming intensity, and noise that is independent of incoming intensity. In our simplified model, θ_c is identical to the intensity-dependent noise, implying $\theta_r(\mathbf{x}) \neq \theta_g(\mathbf{x}) \neq \theta_b(\mathbf{x})$; since, after passing through color filters, non-white light's intensities are different for each color channel. While, ϕ_c is identical to the intensity-independent noise, implying $\phi_r(\mathbf{x}) = \phi_g(\mathbf{x}) = \phi_b(\mathbf{x})$.

Based on the simplified noise model in Equation (15), we can consider that the variance of u in Figure 3.a originates from non-constant values of Λ_c and θ_c. Furthermore, if we extract all pixels that have the same value of u, which means pixels that have the same values of both Λ_c and θ_c (all points inside the vertical line illustrated in Figure 3.a), and project them into the chromaticity intensity space, we will find that the specular and diffuse distributions have the same characteristic, i.e., both of them form curved lines, as shown in Figure 3.b. This is an unexpected characteristic, since we have learned that only specular pixels form curved lines. To understand the diffuse pixels characteristic, further analysis is required.

Diffuse Pixels Distribution Considering the camera noise model, the definition of u for diffuse pixels becomes:

$$u = \frac{m_d(\Lambda_r\theta_r + \Lambda_b\theta_b - 2\Lambda_g\theta_g) + (\phi_r + \phi_b - 2\phi_g)}{m_d(\Lambda_g\theta_g + \Lambda_b\theta_b - 2\Lambda_r\theta_r) + (\phi_g + \phi_b - 2\phi_r)} \quad (16)$$

If we have two pixels, based on the last equation, they will have the same value of u, if their combination of Λ_c and θ_c are identical, since $\phi_r(\mathbf{x}) = \phi_g(\mathbf{x}) = \phi_b(\mathbf{x})$. Moreover, if we focus on ϕ_c, in fact, there are two possible conditions of ϕ_c to produce the same u, namely:

1. $\phi_c^1 = \phi_c^2$
2. $\phi_c^1 \neq \phi_c^2$, but $\Delta_g^1 = \Delta_g^2$ and $\Delta_r^1 = \Delta_r^2$

where $\Delta_g = \phi_r + \phi_b - 2\phi_g$ and $\Delta_r = \phi_g + \phi_b - 2\phi_r$, and the supercript 1 and 2 represent the first and second pixel, respectively.

While the above two conditions produce the same value of u, in the chromaticity-intensity space their distributions are different. The first condition, which means two pixels have identical chromaticity value, will cause the projected points either to occupy the same location in the chromaticity intensity space or to form a vertical distribution due to the different pixel intensities. While, the second condition will causes the projected points of the diffuse pixels to have different locations in chromaticity axis (x-axis). If there are a number of pixels in the second condition, then they will form a curved line distribution, behaving like the projected points of specular pixels (ϕ_c behaves like m_s).

As a result, the presence of the second condition explains the curve lines of diffuse points in chromaticity-intensity space. The number of curved lines in the space is determined by the number of different m_d, and the range of chromaticity values depends on camera noise characteristics which could be different from camera to camera.

Curved Lines Properties For further analysis, we can rewrite the noise model for diffuse pixels as: $I_c(\mathbf{x}) = D_c(\mathbf{x}) + \phi(\mathbf{x})$; where D_c is the combination of the diffuse component and the first type of camera noise (θ_c). Subscript c is removed from ϕ, since its values are identical for all color channels, making ϕ a scalar value. Considering ϕ as a scalar values that vary from pixel to pixel, it becomes more obvious that ϕ behaves like m_s of specular pixel. As a result, we can identify diffuse points in the chromaticity-intensity space using the specular-to-diffuse mechanism. This identification is crucial in estimating diffuse chromaticity.

For specular pixels, we can rewrite the noise model as: $I_c(\mathbf{x}) = D_c(\mathbf{x}) + S_c(\mathbf{x})$; where $S_c = m_s\Gamma_c\theta_c + \phi$. If the difference of θ_c for each color channel is considerably large ($\theta_r \neq \theta_g \neq \theta_b$), the specular component (S_c) will be different for each color channel, even if $\Gamma_r = \Gamma_g = \Gamma_b$. This implies that the specular-to-diffuse mechanism cannot identify the specular curved lines, and thus it benefits us, because we can differentiate them from diffuse curved lines, which means, we become able to identify the diffuse points robustly. Unfortunately, if in case $\theta_r \approx \theta_g \approx \theta_b$ and $\Gamma_r \approx \Gamma_g \approx \Gamma_b$, the mechanism will identify the specular curved lines, and consequently it produces a potential problem in estimating diffuse chromaticity. Subsection 3.3 will discuss the solution of this problem.

Note that, the noise characteristics explained in this section can be found if the camera output is linear to incoming light intensity and $\phi_r \approx \phi_g \approx \phi_b$. In addition, in case a camera does not have the second type of camera noise, the diffuse chromaticity identification becomes more straightforward as the diffuse points will form a vertical line in the chromaticity intensity space.

3.3 Diffuse Pixels Identification

Having characterized the diffuse distribution and identified each of them using the specular-to-diffuse mechanism, we can determine the actual diffuse candidates by choosing a certain point in every diffuse curved line. By assuming ϕ is a positive number, then the actual diffuse pixels (diffuse pixels that are not suffered from the second type of noise) are pixels that have $\phi = 0$. Consequently, the actual diffuse pixels can be chosen from the smallest intensity points (the points that have the biggest chromaticity in each curved line). However, since several curved lines might have no point whose $\phi = 0$, we can not claim that all smallest points in the curved lines to be the actual diffuse pixels; thus, we call them *diffuse candidates*. Figure 4 shows the diffuse candidates from all curved lines of all groups of u.

Choosing diffuse candidates from the lowest intensity of each curved line also enables us to avoid possible problems caused by certain specular distribution (posed in the previous section), namely when $\theta_r \approx \theta_g \approx \theta_b$ and $\Gamma_r \approx \Gamma_g \approx \Gamma_b$, which makes us not able to differentiate the specular points' curved lines from that of the diffuse points. The reason why we can avoid the problem is because most of the lowest intensity of every specular curved line whose S_c is approximately scalar, also ideally indicates the actual diffuse point. In cases where there are specular curved lines that have no diffuse points, we deem them to be outliers whose number is usually smaller than the number of diffuse candidates.

Finally, to obtain a unique value of chromaticity from diffuse pixel candidates, we simply use histogram analysis. Figure 4 illustrates the candidates in chromaticity-intensity

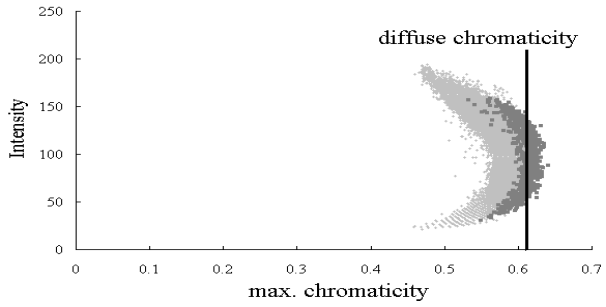

Figure 4: Diffuse candidates amongst input pixels, darker points represent diffuse candidates. Vertical line indicates the single value of diffuse chromaticity obtained using histogram analysis

space and its single estimated diffuse chromaticity.

3.4 Non-White Illumination and Normalization

In the real world, finding a pure-white specular component (S_c) is almost impossible. Most light sources are not wavelength-independent. Moreover, even if the light source is pure white, because of sensor sensitivity and camera noise, the value of the specular component will different for each color channel. Although in this case, the difference is smaller as opposed to non-white illumination.

With this condition, for the first purpose of the mechanism (identifying diffuse candidates), non-white specular components can benefit us, because it makes diffuse candidate identification more robust. Note that the illumination and sensor sensitivity does not affect the second type of noise (ϕ). Thus, we can still identify diffuse pixels whatever the illumination spectral distribution functions may be. In other words, it means that the identification of diffuse candidates under non-white and white illumination is exactly the same.

For the second purpose (reflection components separation: calculating diffuse components of specular pixels), the mechanism requires S_c identical for all channels. Thus, we have to make S_c become a scalar value, which requires normalization process. We propose a simple normalization without using color basis functions, namely, by dividing each pixel's RGB with illumination chromaticity. Color constancy algorithms for uniformly colored surface [13] can be used to estimate the illumination chromaticity.

Having obtained the estimated illumination chromaticity (Γ_c^{est}), the normalized image intensity becomes:

$$\hat{I}_c(\mathbf{x}) = m_d(\mathbf{x})\hat{\Lambda}_c(\mathbf{x}) + m_s(\mathbf{x})\hat{\Gamma}_c(\mathbf{x}) + \hat{\phi}(\mathbf{x}) \tag{17}$$

where $\hat{I}_c(\mathbf{x}) = \frac{I_c(\mathbf{x})}{\Gamma_c^{est}}$; $\hat{\Lambda}_c(\mathbf{x}) = \frac{\Lambda_c\theta_c(\mathbf{x})}{\Gamma_c^{est}}$; $\hat{\Gamma}_c(\mathbf{x}) = \frac{\Gamma_c\theta_c(\mathbf{x})}{\Gamma_c^{est}}$; $\hat{\phi}(\mathbf{x}) = \frac{\phi(\mathbf{x})}{\Gamma_c^{est}}$. Approximately, we can assume $\hat{\Gamma}_c = 1$ and $\hat{\phi} = 0$, and the equation becomes:

$$\hat{I}_c(\mathbf{x}) = m_d(\mathbf{x})\hat{\Lambda}_c(\mathbf{x}) + m_s(\mathbf{x}) \tag{18}$$

Having normalized both input image pixels and diffuse pixels candidates, and then computing the normalized diffuse chromaticity, we can directly separate normalized diffuse and specular components using the specular-to-diffuse mechanism. Finally, in order to obtain the actual diffuse and specular components, we have to renormalize the separated reflection component by multiplying them by the illumination chromaticity (Γ_c^{est}).

4 Experimental Results

This section briefly describes the implementation of the proposed method, and then presents several experimental results on real input images.

Given an input image of uniformly colored surfaces, first, we group the pixels of the image based on their color ratio (u) values. Then, for every group of u, we identify the diffuse candidates. We normalize all diffuse candidates as well as the input image using estimated illumination chromaticity. Based on the normalized diffuse candidates and histogram analysis, we calculate a unique value of the diffuse chromaticity. Having determined the normalized diffuse chromaticity, we separate the normalized input image by using the specular-to-diffuse mechanism, producing normalized diffuse and specular components. Lastly, to obtain the actual components, we multiply both normalized components by the estimated illumination chromaticity.

We have conducted several tests on real images captured using three different CCD cameras: a SONY DXC-9000 (a progressive 3 CCD digital camera), a Victor KY-F70 (a progressive 3 CCD digital camera), and a SONY XC-55 (a monochrome digital camera with external color filters). To estimate illumination chromaticity, we used an illumination chromaticity estimation algorithm [13] and alternatively a white reference from Photo Research Reflectance Standard model SRS-3. As target objects, we used convex objects to avoid interreflection.

Figure 5.a shows characteristics of diffuse pixels affected by camera noise of a Victor KY-F70; the object is a head model image under incandescent light. The darker points indicate the diffuse pixel candidates, and the vertical line is perpendicular to the diffuse chromaticity value. Although there occur some points that, due to ambient light in shadow regions, produce unknown distribution, the diffuse chromaticity is still correctly obtained. Thus, for considerable amount of ambient light, the proposed method is still robust. The separation result of the head model captured using this camera is shown in Figure 5c∼d. The SONY XC-55 camera also has the camera noise characteristic we described as shown in Figure 6.a, and its separation result is shown in Figure 6c∼d. Figure 7.a shows an image of a sandal with high specularity (more than that of the head model) under incandescent light (T=2800 K). Using correct illumination chromaticity, the separation can be done accurately (Figure 7.b and 7.c). Some noise in the upper-right of the sandal is caused by saturated pixels. In the current framework we

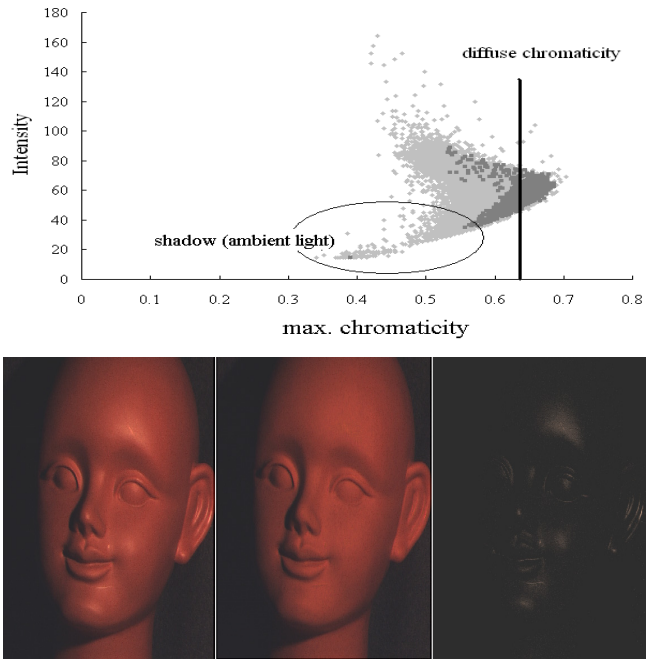

Figure 5: (a) Characteristic of diffuse pixels affected by camera noise of Victor KY-F70 on head model image. (b) Input image (c) diffuse reflection component, (d). specular reflection component

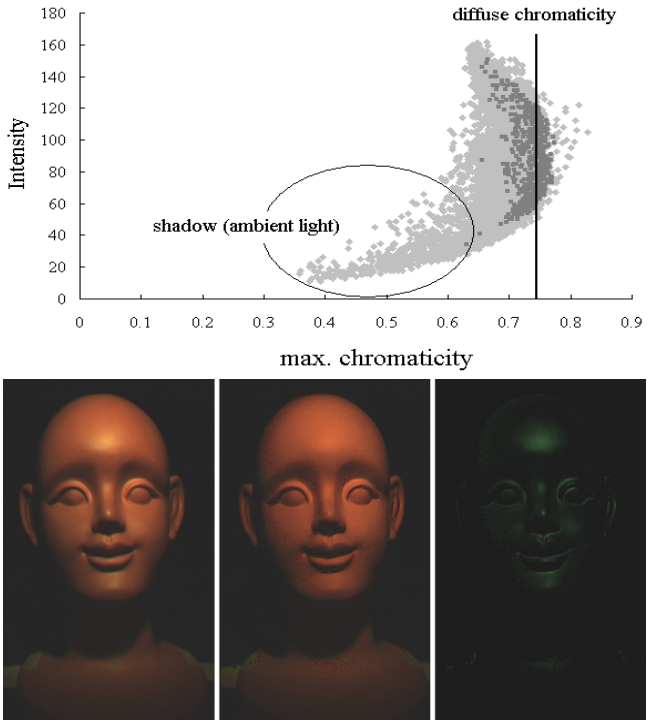

Figure 6: (a) Characteristic of diffuse pixels affected by camera noise of SONY XC-55 on head model image. (b) Input image (c) diffuse reflection component (d) specular reflection component

do not deal with saturated or clipped pixels. Figure 7.d∼f show a head model under multiple incandescent lights and its separation results. Finally, figure 7.g ∼ i show a toy model under solux halogen and its separation results.

5 Conclusion

We have proposed a method to separate diffuse and specular reflection components. Unlike previous methods, our method is principally based on analyzing specular and diffuse pixel distribution in the chromaticity-intensity space, as well as on analyzing noise. To identify diffuse chromaticity and to separate reflection components, we introduced the specular-to-diffuse mechanism. The experimental results on real images taken by several different cameras show that the method is robust for all kinds of surface roughness as well as illumination directions.

Acknowledgements

This research was, in part, supported by Japan Science and Technology (JST) under CREST Ikeuchi Project.

Appendix

Derivation of the correlation between illumination chromaticity and image chromaticity.

$$\sigma_c(\mathbf{x}) = \frac{m_d(\mathbf{x})\Lambda_c + m_s(\mathbf{x})\Gamma_c}{m_d(\mathbf{x})\Sigma\Lambda_i + m_s(\mathbf{x})\Sigma\Gamma_i}$$

For local (pixel based) operation the location $(\mathbf{x})$ can be removed, then:

$$\begin{aligned} \tilde{\sigma} &= \frac{m_d\tilde{\Lambda} + m_s\tilde{\Gamma}}{m_d + m_s} \\ m_s(\tilde{\sigma} - \tilde{\Gamma_c}) &= m_d\tilde{\Lambda} - \tilde{\sigma}m_d \\ m_s &= \frac{\tilde{\sigma}m_d - m_d\tilde{\Lambda}}{\tilde{\Gamma} - \tilde{\sigma}} \end{aligned}$$

Substituting m_s in the definition of I_c with m_s in the last equation:

$$\tilde{I} = m_d(\tilde{\Lambda} - \tilde{\Gamma})(\frac{\tilde{\sigma}}{\tilde{\sigma} - \tilde{\Gamma}})$$

References

[1] R. Bajscy, S.W. Lee, and A. Leonardis. Detection of diffuse and specular interface reflections by color im-

age segmentation. *International Journal of Computer Vision*, 17(3):249–272, 1996.

[2] R. Gershon, A.D. Jepson, and J.K. Tsotsos. Ambient illumination and the determination of material changes. *Journal of Optics Society of America A.*, 3(10):1700–1707, 1986.

[3] G. Healey and R. Kondepudy. Radiometric ccd camera calibration and noise estimation. *IEEE Trans. on Pattern Analysis and Machine Intelligence*, 16(3):267–276, 1994.

[4] G.J. Klinker, S.A. Shafer, and T. Kanade. The measurement of highlights in color images. *International Journal of Computer Vision*, 2:7–32, 1990.

[5] H.C. Lee, E.J. Breneman, and C.P.Schulte. Modeling light reflection for computer color vision. *IEEE Trans. on Pattern Analysis and Machine Intelligence*, 12:402–409, 1990.

[6] S.W. Lee and R. Bajcsy. Detection of specularity using color and multiple views. *Image and Vision Computing*, 10:643–653, 1990.

[7] S. Lin, Y. Li, S. B. Kang, X. Tong, and H.Y. Shum. Diffuse-specular separation and depth recovery from image sequences. pages 210–224, 2002.

[8] S. Lin and H.Y. Shum. Separation of diffuse and specular reflection in color images. In *in proceeding of IEEE Conference on Conference on Computer Vision and Pattern Recognition*, 2001.

[9] S.K. Nayar, X.S. Fang, and T. Boult. Separation of reflection components using color and polarization. *International Journal of Computer Vision*, 21(3), 1996.

[10] J.S. Park and J.T. Tou. Highlight separation and surface orientation for 3-d specular objects. In *in proceeding of IEEE Conference on Conference on Computer Vision and Pattern Recognition*, volume 6, 1990.

[11] Y. Sato and K. Ikeuchi. Temporal-color space analysis of reflection. *Journal of Optics Society of America A.*, 11, 1994.

[12] S. Shafer. Using color to separate reflection components. *Color Research and Applications*, 10, 1985.

[13] R.T. Tan, K. Nishino, and K. Ikeuchi. Illumination chromaticity estimation using inverse-intensity chromaticity space. *in proceeding of IEEE Computer Society Conference on Computer Vision and Pattern Recognition (CVPR)*, pages 673–680, 2003.

[14] L.B. Wolff and T. Boult. Constraining object features using polarization reflectance model. *IEEE Trans. on Pattern Analysis and Machine Intelligence*, 13(7):635–657, 1991.

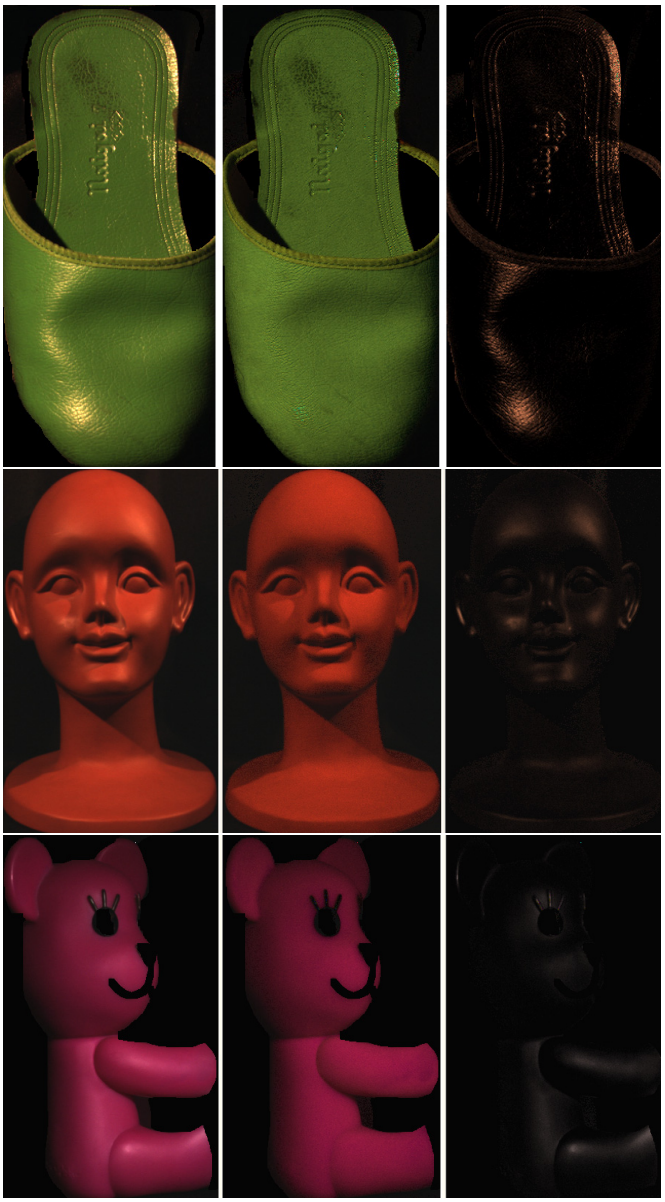

Figure 7: Top row:(a) Input image with high specularity under incandescent light captured using SONY DXC-9000 (b) diffuse reflection component, few noises occur at the right-top of the sandal is due to saturated intensity of the input image (c) specular reflection component; Middle row: (d) Input image with relatively low specularity under multiple incandescent lamps captured using SONY DXC-9000 (e) diffuse reflection component (f) specular reflection component; Bottom row: (g) Input image with very low specularity under solux halogen captured using SONY DXC-9000 (h) diffuse reflection component (i) specular reflection component